An Arnoldi Algorithm for Power-Delivery Networks With Variable Dielectric Constant and Loss Tangent

A. Ege Engin, *Member, IEEE*

***Abstract*—The tracking-sensitivity algorithm is an efficient method to calculate the changes in the network matrix of a circuit, when a global parameter, such as temperature, is continuously varied. In this paper, we apply the concept of tracking sensitivity on the frequency-domain simulation of power-delivery networks (PDNs) in chip packages and printed circuit boards. The global variable we consider is the complex permittivity of the dielectric. We present a methodology to calculate the change in the PDN impedance due to a variation in the dielectric constant, loss tangent, or both. This information is useful not only to understand any deviations between simulations and measurements, but also to understand the impact of the variability of these dielectric properties on the performance of the PDN. Using the tracking-sensitivity algorithm, we can efficiently recalculate the impedance matrix after changing a global parameter. The classical tracking-sensitivity algorithm was based on a power series expansion. This paper presents a more accurate approach based on the block Arnoldi algorithm.**

***Index Terms*—Block Arnoldi, decoupling, ground bounce, power-delivery network (PDN), power-integrity optimization, simultaneous switching noise, target impedance, tracking sensitivity.**

I. Introduction

POWER and ground planes are necessary, in addition to the decoupling capacitors, to reduce the impedance of power-delivery networks (PDNs) on chip packages and printed circuit boards (PCBs). The PDN impedance on a PCB is defined to be between the power and ground planes, as shown in Fig. 1. A low-impedance PDN helps to keep the voltage fluctuations on the nominal dc power level within tolerances, in order for the attached integrated circuits to function properly. Power and ground planes, however, behave as parallel-plate waveguide resonators, exhibiting impedance peaks at antiresonance frequencies. These resonances are undesirable, since they result in increased noise coupling and voltage fluctuations. Typical PDNs are electrically large, have complicated structures for the power and ground planes, and include many decoupling capacitors to maintain a low impedance. Hence, accurate simulation of a PDN typically requires a computationally expensive electromagnetic simulation.

For power-integrity design, locations of the resonance frequencies and the magnitudes of the impedance peaks at those resonances are very important. For power/ground planes, their geometry as well as the dielectric material between them determine the resonance behavior. Hence, it is critical to have accurate information about the dielectric constant and loss tangent, as these parameters affect the impedance. These parameters, however, may change from panel to panel, and even within a panel on fabricated PCBs. Therefore, it is critical to understand the impact of these global variables on the PDN impedance.

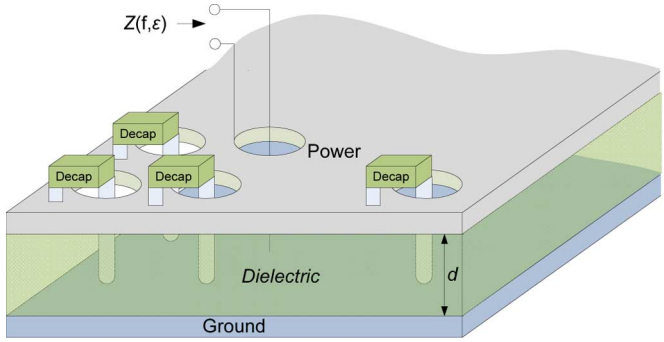

Fig. 1. Decoupling capacitors (decaps) and power/ground planes separated by a thin dielectric with a complex permittivity of ε.

Recently, algorithms for efficient differential and large-change sensitivity calculations of PDN impedance have been developed [1]. These algorithms can efficiently capture the effect of the change in several parameters on the PDN impedance; however, they cannot be applied for a global variable (i.e., a variable that modifies a significant number of elements of the system matrix). For example, the large-change sensitivity algorithm presented in [1] can exactly recalculate the solution after the addition, modification, or relocation of a few decoupling capacitors or a small change in the geometry. However, modification of a global variable, such as the dielectric constant, requires inversion of the system matrix, which is prohibitive for large systems. The tracking-sensitivity algorithm, on the other hand, provides an efficient but approximate answer that matches the first few block moments of the exact solution when a global variable is modified. The presented tracking-sensitivity algorithm, which is applicable for a global variable, has therefore a different purpose and basis than the approach in [1].

In circuit design, calculation of the change in the network matrix due to a variation in a global parameter can be done using various tracking-sensitivity algorithms [2]–[4]. In this paper, we propose a new tracking-sensitivity algorithm, based on a block Arnoldi iteration, that is better suited for the large problems that we will consider. This algorithm is similar to the more recent model-order reduction techniques such as passive reduced-order interconnect macromodeling algorithm (PRIMA) [5]. We

Manuscript received March 26, 2010; revised July 19, 2010; accepted August 9, 2010. Date of publication October 14, 2010; date of current version November 17, 2010.

The author is with the Department of Electrical and Computer Engineering, San Diego State University, CA 92182 USA (e-mail: aengin@mail.sdsu.edu).

Color versions of one or more of the figures in this paper are available online at http://ieeexplore.ieee.org.

Digital Object Identifier 10.1109/TEMC.2010.2075933

apply the tracking-sensitivity approach on electromagnetic simulation of PDNs. For simulation of the PDN, we use the 2-D finite-difference method.

II. Tracking-Sensitivity Algorithm

We are interested in capturing the change in the impedance of a network based on a continuous variation of a global variable. The change in the global variable is denoted by K. In the 2-D finite-difference method, we first build up the nodal admittance matrix $\overline{\overline{Y_N}}$ for the nominal value of the global variable. This results in a matrix equation, which needs to be solved for the given current excitations as

$$\overline{\overline{Y_N}}\,\overline{\overline{V_N}} = \overline{\overline{I}}. \tag{1}$$

The right-hand side is a matrix of size $n \times p$, where the number of ports p is typically much smaller than the total number of internal and external nodes n. We would like to obtain the impedance parameters when the global variable is changed by K. This results in a new matrix equation as

$$(\overline{\overline{Y_N}} + K\overline{\overline{Y_V}})\,\overline{\overline{V}} = \overline{\overline{I}} \tag{2}$$

where the subscripts N and V denote the nominal and variable parts of the nodal admittance matrix, as in [2]. Once (1) is solved for the nominal case, the tracking-sensitivity algorithm allows to solve (2) for a continuous variation in K in an efficient manner. Different algorithms, which are explained in the following, are available for this purpose.

A. Matrix Power Series Method

In the matrix power series method [4], the solution is approximated as

$$\overline{\overline{V}} \approx \sum_{i=0}^{k-1} K^i \overline{\overline{V_i}}. \tag{3}$$

Each term in this summation can be obtained recursively by solving

$$\overline{\overline{Y_N}}\,\overline{\overline{V_{i+1}}} = -\overline{\overline{Y_V}}\,\overline{\overline{V_i}} \tag{4}$$

where the first term is the nominal solution

$$\overline{\overline{V_0}} = \overline{\overline{V_N}}. \tag{5}$$

Since LU decomposition of $\overline{\overline{Y_N}}$ is required only once in (1), and successive iterations in (4) require only forward and backward substitutions, the complexity of computing the coefficients is low. Note the similarity of this approach to the asymptotic waveform evaluation (AWE) method [6]. In AWE, the terms $\overline{\overline{V_i}}$ are called the moments of the frequency response $\overline{\overline{V}}$, where K corresponds to the Laplace variable s. After the calculation of the moments, a Pade approximation is obtained in the AWE method by means of matching the first few moments of a rational function with the matrix power series. The purpose of AWE is to create reduced-order models for efficient time-domain simulation, whereas in the tracking-sensitivity method, we are interested in frequency-domain response and the global variable is a physical property rather than the frequency. More recently, AWE has also been applied for fast frequency sweep in electromagnetic simulations [7], [8]. A 2-D AWE method has also been proposed for simultaneous frequency and permittivity extrapolation in microstrip antennas [9].

B. Eigenvalue Method

The original tracking-sensitivity algorithm [2] was based on solving an eigenvalue problem. Equation (2) can be rewritten as

$$\overline{\overline{V}} = \left(\overline{\overline{1}} + K\overline{\overline{Y_N}}^{-1}\,\overline{\overline{Y_V}}\right)^{-1} \overline{\overline{Y_N}}^{-1}\,\overline{\overline{I}}. \tag{6}$$

The factorization $\overline{\overline{Y_N}}^{-1}\,\overline{\overline{Y_V}} = \overline{\overline{W}}\,\overline{\overline{D}}\,\overline{\overline{W}}^{-1}$, where $\overline{\overline{D}}$ is a diagonal matrix containing the eigenvalues of $\overline{\overline{Y_N}}^{-1}\,\overline{\overline{Y_V}}$ yields

$$\overline{\overline{V}} = \overline{\overline{W}}\left(\overline{\overline{1}} + K\overline{\overline{D}}\right)^{-1} \overline{\overline{W}}^{-1}\overline{\overline{Y_N}}^{-1}\,\overline{\overline{I}}. \tag{7}$$

Since $(\overline{\overline{1}} + K\overline{\overline{D}})$ is a diagonal matrix, its inverse can be obtained analytically providing an exact solution for $\overline{\overline{V}}$ in the form of a partial fraction expansion of the variable K [2], [10]. This form of tracking sensitivity is not suitable for large systems, since it requires the computation and storage of all of the eigenvalues and eigenvectors. Another approach based on the calculation of determinants has been proposed in [3], which however, is also not suitable for large systems. Next, we propose a new approach for large systems based on the block Arnoldi iteration.

C. Block-Arnoldi-Based Tracking-Sensitivity Algorithm

In the block Arnoldi method, instead of calculating an exact solution $\overline{\overline{V}}$ using the eigenvalues and eigenvectors of $\overline{\overline{Y_N}}^{-1}\,\overline{\overline{Y_V}}$, we find an approximation to the solution. This is accomplished by the factorization

$$-\overline{\overline{Y_N}}^{-1}\,\overline{\overline{Y_V}} = \overline{\overline{X}}\,\overline{\overline{H}}\,\overline{\overline{X}}^{H} \tag{8}$$

where $\overline{\overline{X}}$ is a unitary matrix and $\overline{\overline{H}}$ is an upper Hessenberg matrix. With the definitions

$$\overline{\overline{A}} = -\overline{\overline{Y_N}}^{-1}\overline{\overline{Y_V}} \tag{9}$$

and

$$\overline{\overline{R}} = \overline{\overline{Y_N}}^{-1}\overline{\overline{I}} \tag{10}$$

$\overline{\overline{X}}$ orthogonalizes the Krylov subspace defined by the column space of $[\overline{\overline{R}}\ \overline{\overline{AR}}\ \overline{\overline{A}}^2\overline{\overline{R}},\ \ldots,\ \overline{\overline{A}}^{k-1}\overline{\overline{R}}]$. Similar to (7), we obtain an approximation to the solution in terms of

$$\overline{\overline{V}} \approx \overline{\overline{X}}\left(\overline{\overline{1}} - K\overline{\overline{H}}\right)^{-1} \overline{\overline{X}}^{H}\,\overline{\overline{R}} \tag{11}$$

which can be expressed as a partial fraction expansion after diagonalization of $\overline{\overline{H}}$, which is a small square matrix of size $kp \times kp$. The approximate solution matches the first k block moments of the exact solution [11]. This approach numerically provides more accurate results compared to the matrix power series approach, since the power iteration in (4) converges to an eigenvector associated with the largest eigenvalue [10], and

Algorithm 1. Block Arnoldi Algorithm for Complex Matrices

1 $\overline{\overline{X}}_1 = QR(\overline{\overline{Y_N}}^{-1}\overline{\overline{I}})$
2 for $i = 1, \ldots, k-1$
3 $\quad \overline{\overline{X}}_{i+1} = \overline{\overline{Y_N}}^{-1}\overline{\overline{Y_V X}}_i$
4 $\quad$ for $j = 1, \ldots, i$
5 $\quad\quad \overline{\overline{H}}_{j,i} = \overline{\overline{X}}_j^H \overline{\overline{X}}_{i+1}$
6 $\quad\quad \overline{\overline{X}}_{i+1} = \overline{\overline{X}}_{i+1} - \overline{\overline{H}}_{j,i}\overline{\overline{X}}_j$
7 $\quad$ end for
8 $\quad [\overline{\overline{X}}_{i+1}, \overline{\overline{H}}_{i+1,i}] = QR(\overline{\overline{X}}_{i+1})$
9 end for
10 $\overline{\overline{H}}_{:,k} = \overline{\overline{X}}^H \overline{\overline{Y_N}}^{-1}\overline{\overline{Y_V}}\,\overline{\overline{X}}_k$
11 $\overline{\overline{H}} = -\overline{\overline{H}}$

hence cannot recover information about other eigenvalues of the system for even small values of k.

We modify the block Arnoldi algorithm presented in [5], as shown in Algorithm 1. Note the following remarks on this algorithm.

1) The matrices we are considering are in general complex in contrast to the real matrices that are involved in model order reduction of RLC circuits. Hence, we use the conjugate transpose denoted by the superscript H instead of the transpose.
2) The inner *for* loop can be iterated multiple times to improve orthogonality down to machine precision [5].
3) Since Arnoldi stops at $i = k-1$, the last block column of $\overline{\overline{H}}$ is computed using step 10.
4) We keep the same sign notation, as in [5], which performs Arnoldi on $-\overline{\overline{A}}$ and not on $\overline{\overline{A}}$. To obtain the correct sign, step 11 is necessary, as pointed out in [12].
5) The QR decomposition is calculated only for the first N orthogonal vectors. In case $\overline{\overline{I}}$ is a single vector, the QR decomposition in steps 1 and 8 reduces to a simple vector normalization. Since we are not interested in a macromodel, but rather the tracking sensitivity, it is also possible to apply the Arnoldi algorithm for each right-hand-side vector of $\overline{\overline{I}}$ separately. This would also eliminate the need to consider the gradual exact deflation [13] due to linearly dependent vectors in the Krylov subspace.
6) The algorithm we present has matrix indices that consistently start at 1.

In the next section, we present briefly how the matrices $\overline{\overline{Y_N}}$ and $\overline{\overline{Y_V}}$ are formed in case of PDN simulations.

III. Analysis of Power/Ground Planes and Decoupling Capacitors

Consider the power/ground planes on a chip package or PCB, as shown in Fig. 1. An efficient way of calculating the impedance profile of this structure can be developed based on the 2-D finite-difference method [14], [15]. We make use of the fact that the thickness of the dielectric is much smaller than the lateral dimensions, hence the variation of the electric and magnetic fields with respect to the vertical z-direction can be neglected. Then, assuming that there are no decoupling capacitors for the time being, the voltage $u(x, y)$ at any point $P(x, y)$ can be described with the 2-D Helmholtz wave equation

$$\nabla^2 u + k^2 u = -jJ_z \omega \mu d \tag{12}$$

where k is the wave number, J_z is the current density in the vertical direction, ω is the angular frequency, μ is the permeability, and d is the dielectric thickness. The boundary conditions are of Neumann type for the planes, which can have arbitrary borders or cut-outs. The five-point finite-difference discretization of the Laplace operator (∇^2) in (12) yields an equivalent circuit representation, as shown in Fig. 2 [14]–[16], where

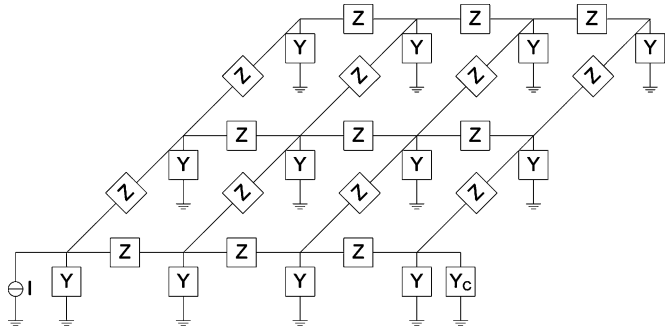

Fig. 2. Equivalent circuit representation for the example of a rectangular-shaped power/ground plane pair with a discretization of 4×3. A current source is connected to the lower left node and a decap is connected to the lower right node.

$$Z = j\omega\mu d + 2\sqrt{\frac{j\omega\mu}{\sigma}}\coth(t\sqrt{j\omega\mu\sigma}) \tag{13}$$

$$Y = j\omega\varepsilon\frac{h^2}{d} \tag{14}$$

where σ is the conductivity of the planes, t is the thickness of each plane, ε is the complex permittivity of the dielectric, and h is mesh length [16]. To incorporate the effect of copper surface roughness, an effective conductivity that is a function of surface roughness and skin depth can be used [17]. The nodal admittance matrix $\overline{\overline{Y_N}}$ of the equivalent circuit model in Fig. 2 can be built-up as

$$\overline{\overline{Y_N}}\,\overline{\overline{V}} = \overline{\overline{I}} \tag{15}$$

where each column of $\overline{\overline{V}}$ is a vector of node voltages for the corresponding current excitations on the same column of $\overline{\overline{I}}$. Solution of this matrix equation provides the distribution of voltage for any current excitation, which is equivalent to the self and transfer impedances assuming a current excitation of 1 A at a single node for each column of $\overline{\overline{I}}$. To build-up $\overline{\overline{Y}}$, each shunt admittance at node p is added as

$$\begin{bmatrix} \ddots & & \\ \cdots & Y & \cdots \\ & & \ddots \end{bmatrix} \begin{bmatrix} \vdots \\ V_p \\ \vdots \end{bmatrix} = \begin{bmatrix} \vdots \\ I_p \\ \vdots \end{bmatrix} \tag{16}$$

whereas, each series impedance between nodes p and q is added as

$$\begin{bmatrix} \ddots & & & & \\ \cdots & \frac{1}{Z} & \cdots & -\frac{1}{Z} & \cdots \\ & & \ddots & & \\ \cdots & -\frac{1}{Z} & \cdots & \frac{1}{Z} & \cdots \\ & & & & \ddots \end{bmatrix} \begin{bmatrix} \vdots \\ V_p \\ \vdots \\ V_q \\ \vdots \end{bmatrix} = \begin{bmatrix} \vdots \\ I_p \\ \vdots \\ I_q \\ \vdots \end{bmatrix}. \quad (17)$$

The decoupling capacitors are simply included in the matrix as additional shunt admittances with the admittance

$$Y_C = \frac{1}{1/(j\omega C) + j\omega L + R} \quad (18)$$

based on a series RLC model for the decoupling capacitor. Hence, the addition of a decoupling capacitor merely corresponds to the addition of its admittance on the corresponding diagonal element of the nodal admittance matrix, as in (16).

IV. Tracking Sensitivity for the Complex Permittivity

Assume that we have assembled the nodal admittance matrix $\overline{\overline{Y_N}}$ for a nominal value of the complex relative permittivity ε_r, where $\varepsilon = \varepsilon_r \varepsilon_0$. Since there is a constant shunt admittance Y to ground at each node, and the global variable ε_r only affects that admittance, we can express the nodal admittance matrix, when the complex relative permittivity is changed by $\Delta\varepsilon$ as

$$\left(\overline{\overline{Y_N}} + \Delta\varepsilon j\omega\varepsilon_0 \frac{h^2}{d}\overline{\overline{1}}\right) \overline{\overline{V}} = \overline{\overline{I}}. \quad (19)$$

Comparing (19) with (2) yields

$$K = \Delta\varepsilon \quad (20)$$

and

$$\overline{\overline{Y_V}} = j\omega\varepsilon_0 \frac{h^2}{d}\overline{\overline{1}}. \quad (21)$$

Hence, we can apply the Arnoldi-based tracking-sensitivity algorithm presented in Section II. Note that the complex relative permittivity is in the form of

$$\varepsilon_r = \varepsilon_r'(1 - j\tan\delta) \quad (22)$$

where ε_r' is the dielectric constant. Hence, we can account for changes in the dielectric constant, loss tangent, or in both of these parameters, once the tracking-sensitivity algorithm is applied to obtain the approximate model. Also, $\overline{\overline{Y_V}}$ is an identity matrix (scaled with a constant); therefore, several matrix–matrix products in the Arnoldi algorithm (in steps 3 and 10) reduce to scalar-matrix products.

V. Numerical Results

A. Square-Shaped Plane Pair

A 2 cm × 2 cm square-shaped board is simulated with the nominal dielectric constant of 4.0, and loss tangent of 0.01. The dielectric thickness is 200 μm, and two ports are defined on two diagonally opposite corners of the board. The mesh length is chosen as 0.2 mm. Planes are made of copper with a thickness of 35 μm. Using the tracking-sensitivity algorithm with an order of $k = 7$, the simulation is repeated for a dielectric constant of 4.5, and loss tangent of 0.025. The new simulation result is also compared with the simulation that was started from scratch, which is denoted as "exact result" in Fig. 3. In order to quantify the comparison of data, the feature selective validation (FSV) technique [18] has been applied. Between the "tracking sensitivity" and the "exact result", all three figures of merit of the FSV method (i.e., the ADM, FDM, and GDM measures) had a grade and spread value of "excellent". For comparison, between the "nominal simulation" and "exact result" for the magnitude of $Z12$, grade value was "poor," whereas the spread value was "fair" to "poor". Hence by applying the tracking-sensitivity algorithm, the poor agreement has been improved to an excellent agreement with the exact result.

The accuracy of the tracking-sensitivity algorithm decreases if it is applied using fewer block moments (k), larger frequency range, or larger change in the global variable (K). As an example, the tracking-sensitivity algorithm only provides a "fair" grade and spread in FSV figures of merit for the magnitude of $Z12$, if the order of approximation is $k = 2$.

B. Power Island

Power islands have been proposed to provide reduction in noise coupling between various areas of a power plane in [19]. One example is shown in Fig. 4, which is one of the cases discussed in [1]. The dielectric thickness of the test structure is 117 μm. In the nominal simulation, the dielectric constant was assumed to be 5.0, and the loss tangent was assumed to be 0. As these values do not represent the correct dielectric parameters, the nominal results do not match the measurement results, as shown in Fig. 5. Using the tracking-sensitivity algorithm, the transfer impedance has been recalculated using a dielectric constant of 4.1, and loss tangent of 0.02. The tracking-sensitivity result now agrees well with the measurements.

The results can be recalculated for any value of the loss tangent and dielectric constant with much smaller computational complexity compared to restarting the simulation from scratch. Hence, tracking sensitivity becomes an efficient approach to fit simulation results to measurement results; or to consider the effect of the frequency-dependent complex permittivity on PDN impedance. In order to fit simulation results to measured data, the dielectric constant and loss tangent need to be iteratively adjusted. If the fitting is done manually, it should be kept in mind that the dielectric constant mainly influences the locations of the resonance frequencies, whereas the loss tangent mainly influences the magnitude of the impedance peaks. Also, since the complex permittivity is now a variable, simulations can be efficiently repeated for any frequency-dependent variation of the dielectric constant and loss tangent.

In this example, the order of the model was $k = 15$. In general, a larger k is required as the deviation between the nominal simulation and recalculation gets larger. For most purposes, the nominal dielectric parameters would be closer to the updated parameters, compared to the example considered here; hence, $k = 15$ would be sufficient.

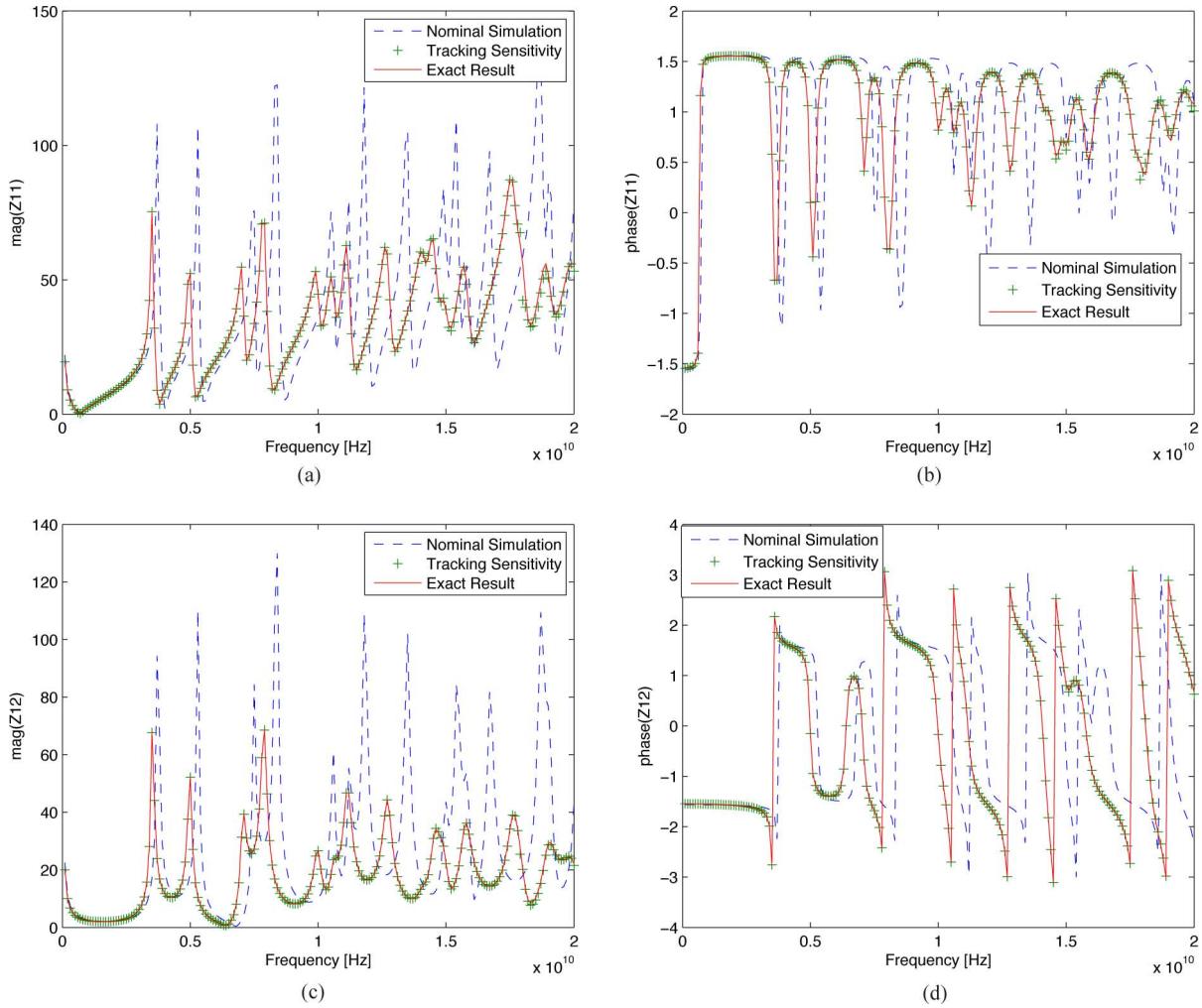

Fig. 3. Simulations based on tracking sensitivity for a 2 cm × 2 cm square-shaped board.

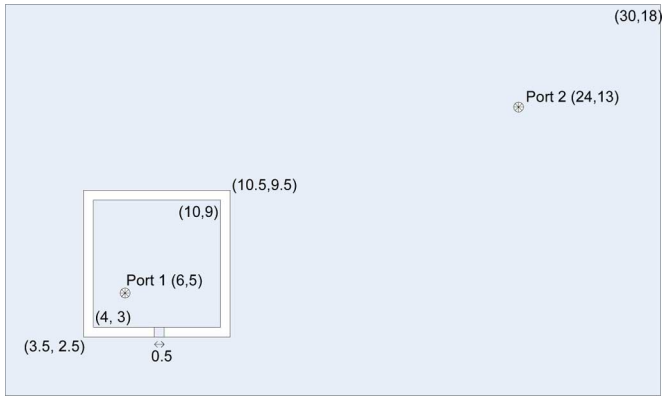

Fig. 4. Geometry of the power island and the bridge with a width of 0.5 mm connected to the center of the power island's bottom edge. All units are in mm.

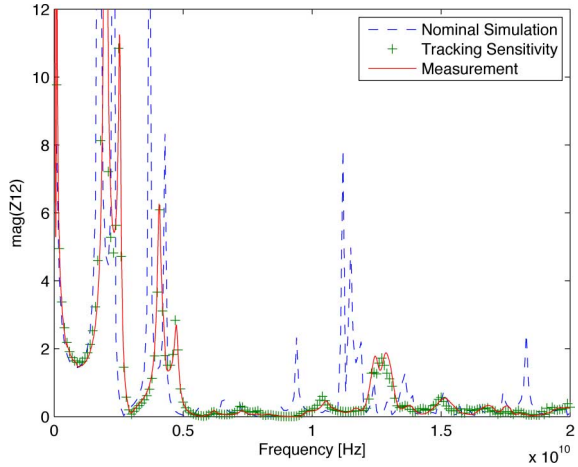

Fig. 5. Measured and simulated transfer impedance using the tracking-sensitivity algorithm for $\varepsilon_r' = 4.1$ and $\tan\delta = 0.02$, whereas the nominal case was simulated for $\varepsilon_r' = 5.0$ and $\tan\delta = 0$.

To demonstrate the efficiency of the tracking-sensitivity algorithm, this example was run at a single frequency point with a fine discretization resulting in about 0.3M unknowns. The standard solution [i.e., the direct solution of (1)] took 14.6 s, whereas the Arnoldi iteration shown in Algorithm 1 took 14.7 s (assuming that the LU decomposition is already available from the direct solution) on a laptop PC with 3 GB of RAM and a clock frequency of 1.4 GHz. Once the Arnoldi iteration was complete, each additional simulation for a different value of the

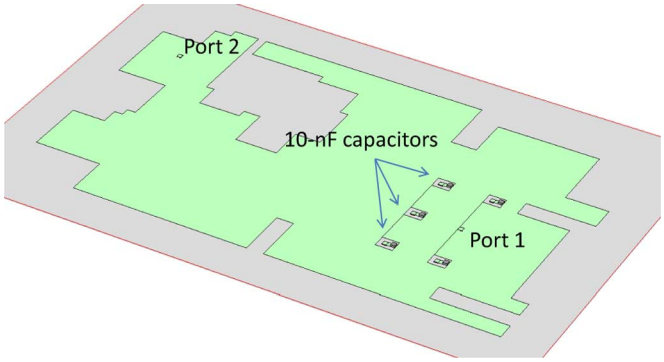

Fig. 6. A 14.5 cm × 8.5 cm board including five 10-nF decoupling capacitors.

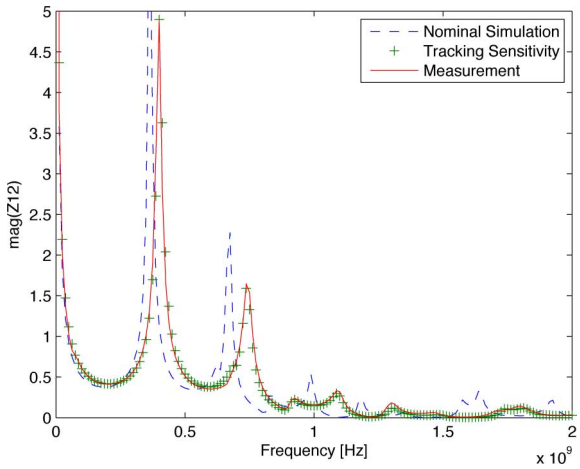

Fig. 7. Application of the tracking-sensitivity algorithm for the board shown in Fig. 6 without the decaps.

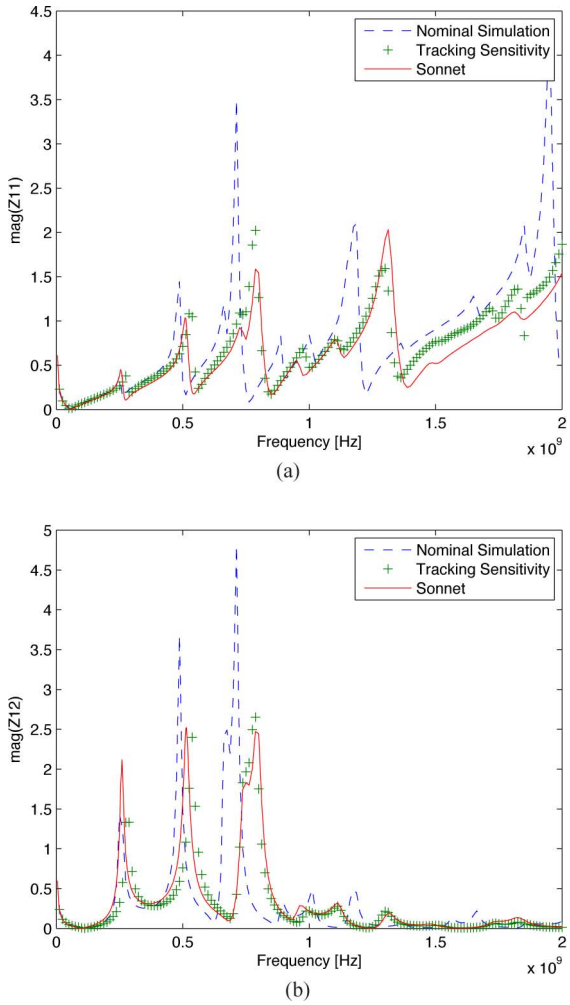

Fig. 8. Application of the tracking-sensitivity algorithm for the board shown in Fig. 6 with the decaps.

complex permittivity [i.e., calculation of (11)] took 0.7 s using the tracking-sensitivity algorithm. Hence, the initial Arnoldi iteration took about the same time as the standard solution, but afterward, there was a speed up of about 20X for each simulation with a different complex permittivity.

C. Board With Decoupling Capacitors

Next, we consider the board shown in Fig. 6, which includes five 10-nF decoupling capacitors to suppress the coupling between ports 1 and 2. The total board size is 14.5 cm × 8.5 cm.

First, the transfer impedance of the bare board was measured. In nominal simulation, the dielectric constant was 5.0 and the loss tangent was 0. Note that it is not necessary to choose the nominal loss tangent to be zero. We choose a zero loss tangent to demonstrate the accuracy of the tracking-sensitivity algorithm for a large variation of the global parameter. Using the tracking-sensitivity algorithm, we adjusted the dielectric constant and loss tangent to $\varepsilon_r' = 4.1$ and $\tan\delta = 0.02$. By adjusting the complex permittivity, a very good match is obtained between simulation and measurements, as shown in Fig. 7.

Next, this structure including the decoupling capacitors was simulated with a full-wave electromagnetic solver, Sonnet[1], where the decoupling capacitors were added as ideal lumped components. In the 2-D finite-difference method, the via and pad inductance and resistance was included as 150 pH and 10 mΩ. In Sonnet simulation, the dielectric constant was 4.1 and the loss tangent was 0.02. As it can be seen in Fig. 8, the tracking-sensitivity result based on the nominal simulation agrees well with Sonnet results. For the nominal simulation, once again we started with $\varepsilon_r' = 5.0$ and $\tan\delta = 0$. This examples demonstrates that the tracking-sensitivity algorithm can be applied also in the presence of decoupling capacitors.

VI. Conclusion

This paper presents a new tracking-sensitivity algorithm based on Arnoldi iteration. We apply the tracking sensitivity for efficient simulation of PDN impedances, where the complex permittivity of the dielectric is variable. With this approach, after an initial Arnoldi iteration using the nominal value of

[1]Sonnet 12.54, Sonnet Software Inc.

the complex permittivity, we can rapidly generate simulation results for different values of the dielectric constant and loss tangent. The Arnoldi-based tracking sensitivity was observed to be accurate to reproduce the PDN impedance for a typical PCB substrate, even when the nominal simulation was done for a lossless substrate. Simultaneously, the dielectric constant was varied by more than 10%, without affecting the accuracy. Each new simulation provided a speed-up of about 20X compared to starting the simulation from scratch for a given example.

The presented approach is suitable in power-integrity simulation of PDNs in applications, such as fitting the permittivity used in simulations to match measurement data, or investigating various frequency-dependent permittivity models and their effects on power integrity.

REFERENCES

[1] A. Engin, "Efficient sensitivity calculations for optimization of power delivery network impedance," *IEEE Trans. Electromagn. Compat.*, vol. 52, no. 2, pp. 332–339, May 2010.

[2] K.-H. Leung and R. Spence, "Tracking sensitivity: An efficient algorithm for linear nonreciprocal circuits," *Electron. Lett.*, vol. 10, no. 18, pp. 377–378, Sep. 5, 1974.

[3] P. Bryant, "Tracking sensitivity: An alternative algorithm for linear nonreciprocal circuits," *Electron. Lett.*, vol. 11, no. 5, pp. 114–116, Mar. 6, 1975.

[4] T. Neumann and D. Agnew, "Tracking sensitivity: A practical algorithm," *Electron. Lett.*, vol. 13, no. 12, pp. 371–372, Jun. 9, 1977.

[5] A. Odabasioglu, M. Celik, and L. Pileggi, "Practical considerations for passive reduction of RLC circuits," in *1999 Proc. IEEE/ACM Int. Conf. Comput.-Aided Des., Dig. Tech. Papers*, pp. 214–219.

[6] L. Pillage and R. Rohrer, "Asymptotic waveform evaluation for timing analysis," *IEEE Trans. Comput.-Aided Des. Integr. Circuits Syst.*, vol. 9, no. 4, pp. 352–366, Apr. 1990.

[7] M. Li, Q.-J. Zhang, and M. Nakhla, "Finite difference solution of em fields by asymptotic waveform techniques," in *Proc. Inst. Elect. Eng. (IEE) Microw., Antennas Propag.*, vol. 143, no. 6, pp. 512–520, Dec. 1996.

[8] G. Ogucu, "Hybrid use of AWE with spatial matrix interpolation in the analysis of printed structures," *IEEE Microw. Wireless Compon. Lett.*, vol. 19, no. 2, pp. 68–70, Feb. 2009.

[9] Y. Xiong, D. Fang, and F. Ling, "Two-dimensional AWE technique in fast calculation of microstrip antennas," in *Proc. 3rd Int. Conf. Microw. Millimeter Wave Technol. (ICMMT)*, Aug. 2002, pp. 393–396.

[10] P. Feldmann and R. Freund, "Efficient linear circuit analysis by Pade approximation via the Lanczos process," *IEEE Trans. Comput.-Aided Des. Integr. Circuits Syst.*, vol. 14, no. 5, pp. 639–649, May 1995.

[11] A. Odabasioglu, M. Celik, and L. Pileggi, "Prima: Passive reduced-order interconnect macromodeling algorithm," *IEEE Trans. Comput.-Aided Des. Integr. Circuits Syst.*, vol. 17, no. 8, pp. 645–654, Aug. 1998.

[12] S. Aaltonen and J. Roos, "Simple reduced-order macromodels with PRIMA," in *Proc. 9th Int. Conf. Electron., Circuits Syst., 2002*, vol. 1, pp. 367–370.

[13] R. Freund, "Passive reduced-order modeling via Krylov-subspace methods," in *Proc. IEEE Int. Symp. Comput.-Aided Control Syst. Des. (CACSD) 2000*, pp. 261–266.

[14] O. Ramahi, V. Subramanian, and B. Archambeault, "A simple finite-difference frequency-domain (FDFD) algorithm for analysis of switching noise in printed circuit boards and packages," *IEEE Trans. Adv. Packag.*, vol. 26, no. 2, pp. 191–198, May 2003.

[15] T. Tarvainen, "Simplified modeling of parallel plate resonances on multilayer printed circuit boards," *IEEE Trans. Electromagn. Compat.*, vol. 42, no. 3, pp. 284–289, Aug. 2000.

[16] M. Swaminathan and A. E. Engin, *Power Integrity Modeling and Design for Semiconductors and Systems*. Upper Saddle River, NJ: Prentice Hall Press, 2007.

[17] H. Braunisch, X. Gu, A. Camacho-Bragado, and L. Tsang, "Off-chip rough-metal-surface propagation loss modeling and correlation with measurements," in *Proc. 57th Electron. Compon. Technol. Conf. (ECTC)' 2007*, May 29–Jun. 1, 2007, pp. 785–791.

[18] A. Duffy, A. Martin, A. Orlandi, G. Antonini, T. Benson, and M. Woolfson, "Feature selective validation (FSV) for validation of computational electromagnetics (CEM)—Part I: The FSV method," *IEEE Trans. Electromagn. Compat.*, vol. 48, no. 3, pp. 449–459, Aug. 2006.

[19] W. Cui, J. Fan, H. Shi, and J. Drewniak, "DC power bus noise isolation with power islands," in *Proc. IEEE Int. Symp. Electromagn. Compat. (EMC) 2001*, vol. 2, pp. 899–903.

A. Ege Engin (M'05) received the B.S. degree from Middle East Technical University, Ankara, Turkey, the M.S. degree from the University of Paderborn, Paderborn, Germany, both in electrical engineering, in 1998 and 2001, respectively, and the Ph.D. degree with Summa Cum Laude from the University of Hannover, Hannover, Germany, in 2004.

He was as a Research Engineer at the Fraunhofer-Institute for Reliability and Microintegration, Berlin, Germany. From 2006 to 2008, he was an Assistant Research Director of the Microsystems Packaging Research Center at Georgia Tech. He is currently an Assistant Professor in the Department of Electrical and Computer Engineering, San Diego State University, CA. He is the author or coauthor of more than 70 publications in journals and conferences in the areas of signal and power-integrity modeling and simulation, 1 patent, and 3 patent applications. He is also the coauthor of the book "Power Integrity Modeling and Design for Semiconductors and Systems," published by Prentice Hall in 2007.

Dr. Engin is the recipient of the Semiconductor Research Corporation Inventor Recognition Award in 2009. He has coauthored publications that received the Outstanding Poster Paper Award in the Electronic Components and Technology Conference (ECTC) 2006, Best Paper Award Finalist in the Board-Level Design Category at DesignCon 2007, and Best Paper of the Session Award in IMAPS Advanced Technology Workshop on RF and Microwave Packaging 2009.